JMEPEG
https://doi.org/10.1007/s11665-019-04105-z

1059-9495/$19.00

Interaction of Guided Waves with Delamination in a Bilayered Aluminum-Composite Pressure Vessel

Mauro Parodi, Cosima Fiaschi, Vittorio Memmolo, Fabrizio Ricci, and Leandro Maio

(Submitted October 10, 2018; in revised form March 16, 2019)

Composite structures are likely affected by barely visible or not visible damages including delaminations, disbondings or detachments among several parts connected together to obtain the whole structure. Pressure vessels adopted for space application represent a significant case. They are designed with a metal to composite hybrid configuration. The harsh and unpredictable missions may threaten the connection between different materials inducing hidden damage. Guided ultrasonic waves are investigated in this work in view of detection and assessment of small emerging flaws at the interface level. Experimental and numerical approaches are used to predict the propagation behavior of the first antisymmetric (A_0) Lamb wave mode. That is complicated by the interaction with the connected area, the multimodal behavior and the interaction with damage when present. However, the work demonstrates that simplified models can be used to investigate the wave field accurately with a fewer computational effort possible. Finally, theoretical considerations and numerical outcomes are used in combination to reveal the interaction phenomena and demonstrate the detection capability of A_0 mode for a possible damage index approach.

Keywords Aerospace structures, Composites, Damage detection, Hybrid structures, Numerical simulation, Wave propagation

1. Introduction

Composite structures have been increasingly adopted in the aerospace field to enhance the overall performances of the vehicles. Depending upon the type of application, they are differently designed with the usual aim to decrease the weight and/or increase the payload. Pressure vessels adopted for space applications represent a significant case. They are designed with an inner cylindrical hull made of high-performance aluminum alloy covered by a thick carbon-based composite clad to reduce the overall weight of the whole hollow container. Since they are likely employed in harsh and unpredictable condition, the interface between metallic and composite parts is maintenance critical. Hence, it is worth monitoring a possible detachment which may be mission threatening.

Structural Health Monitoring (SHM) techniques can be adopted for the latter aim using several sensors permanently attached on to the structure. They usually monitor the hosting structure in terms of vibration response (Ref 1, 2), electromechanical impedance (Ref 3) or wave propagation (Ref 4). Due to their capability to interrogate relatively thin structures, guided waves are efficiently adopted to detect small emerging flaws within composites which are typically induced by low-velocity impacts and which are barely visible during visual inspection (Ref 5). GW-based SHM techniques have been increasingly considered with respect to conventional nondestructive techniques. Although the latter ones are strongly improved in terms of damage characterization (Ref 6), the continuous monitoring of the structure has a promising impact on the operative costs of aircrafts (Ref 7). Likewise, in the last years such a scenario is appearing even in space applications (Ref 8). In addition, while aircraft structures can be more easily monitored when the aircraft is not in service, space vehicles need a continuous monitoring process in order to assess the structural integrity during the mission being impossible releasing the component from service.

Lamb wave propagation for damage detection has been massively investigated in the last decades leading to a wide number of techniques. They generally include linear (Ref 9) and nonlinear (Ref 10, 11, 12) techniques or a combination of both approaches (Ref 13). The propagation footprint is mostly investigated to detect the presence of damage (Ref 14), localize its position when present (Ref 15, 16) and even characterize its severity (Ref 17, 18). Damage evolution can be also monitored investigating how the waves behave after load cycles (Ref 19, 20). Guided waves are generally interacting with any type of damage where the wavelength is comparable or shorter than the emerging defect. At that location, the discontinuity induces the scattering of propagating modes (Ref 21), their conversion into similar (Ref 22) or different (Ref 23) modes and trapped waves may even appear (Ref 24). That is where linear and nonlinear phenomena are scattering and can be captured by sensors opportunely located. Intercepting this complex behavior allows damage detection in such a reverse approach, where the propagation feature warns the damage which has induced the wave to behave in such a certain manner. On the other hand,

This article is an invited submission to JMEP selected from presentations at the International Symposium on Dynamic Response and Failure of Composite Materials (Draf2018) held June 12-15, 2018, on the Island of Ischia, Italy, and has been expanded from the original presentation.

Mauro Parodi and **Cosima Fiaschi**, EXEMPLAR SRL, C.So Vittorio Emanuele II, 161, 10139 Turin, Italy; **Vittorio Memmolo, Fabrizio Ricci,** and **Leandro Maio**, Department of Industrial Engineering – Aerospace Section, Università degli Studi di Napoli Federico II, Via Claudio 21, 80125 Naples, Italy. Contact e-mails: mauro.parodi@exemplar.com and vittorio.memmolo@unina.it.

Published online: 17 May 2019

such complexities need for a comprehensive understating of wave propagation in composite media. The knowledge of interaction phenomena can be used whether to compensate some phenomena existing due to geometry (Ref 25), material inhomogeneity (Ref 26), temperature (Ref 27) and environmental disturbances (Ref 28), or to develop model-based techniques (Ref 29).

The need of understanding how the waves behave while traveling within composite components highlighted the role of numerical approaches. Virtual environments can be used to intercept a specific phenomenon or even quantify the system performances in a model-based estimation. Generally, numerical simulations can strongly aid SHM development. Various techniques have been increasingly developed to simulate the wave propagation in solid media. Those include the classic finite element modeling (FEM), combined analytical FEM approaches (Ref 30), wave finite element approach (Ref 10, 31), spectral finite element modeling (Ref 32, 33) and other advanced techniques (Ref 34). Among them, FEM is widely adopted for complex physical problems (Ref 35, 36) and likely embedded in commercial software, allowing an easy manipulation and a good compromise between efficiency and accuracy. While considering composite structures, different approaches are available in the literature to simulate wave propagation. They are broadly divided into three-dimensional (3D), equivalent single layer (ESL) and two-dimensional (2D) approaches. The 3D and ESL discretization techniques consider the whole structure. The section is discretized accurately as a multilayered solid or with a single layer whose stiffness is equivalent to that of the whole section, respectively (Ref 26). Instead, the 2D approach discretizes the section accurately through the thickness while the lateral dimension is considered as infinite medium (Ref 37). The former approaches correctly represent the in-plane propagation. However, the ESL approach comes to a strong approximation through the thickness. That is where the 2D approach differs from the ESL technique, reducing the analysis along one direction of propagation only. In this case, both transient dynamics and modal analysis are adopted to reveal the propagation behavior in undamaged structures (Ref 37). Instead, the dynamic transient analysis is usually adopted to simulate the wave propagation in damaged structures (Ref 38). Although the 3D approach returns a high-fidelity response of the structure, it requires high computational costs while increasing the number of layers or the frequency. On the contrary, the ESL and 2D approaches strongly reduce the number of degree of freedoms at the cost of a likely less accuracy. However, the latter consideration is strictly connected to the specific problem and it remains an open question in the literature.

In a joined research project led by Thales Alenia Space, the present work shows the application of guided waves with the support of simulation models to perform SHM on a composite overwrapped pressure vessel (COPV). The complex structure is first discretized to accurately model impact and wave propagation behavior employing high-fidelity 3D approach. Then, different techniques are employed to reduce the computational efforts in view of achieving a cost-effective virtual framework to simulate wave propagation and look into the wave damage interaction. Finally, the damage presence is investigated by validated 2D model simulation. The feasibility of GW-based SHM for the continuous monitoring of the COPV structure and the interaction phenomena are thus revealed and discussed.

2. Statement of the Problem

The COPV is a component commonly used in space structures or launch vehicles to serve as an air or, more generally, any fluid container. It is a multilayered component enclosing an aluminum *Al6061-T6* liner covered by a carbon fiber-reinforced plastic (CFRP) manufactured using filament winding (FW) technology. An epoxy adhesive layer is interposed between the liner and the composite shell. The aluminum liner has the purpose of containing the pressurized fluid without leakage. Meanwhile, the external wrapping provides structural strength to the component and it serves as a protection against impact as well. The resulting structure is characterized by high strength and low weight. The full scale of the liner and the whole container considered in the present work are shown in Fig. 1(a) and (b), respectively.

The composite tow is a unidirectional pre-preg made of Toray T1000™ fiber and Hexcel M10™ epoxy resin. The layup is composed by the winding of tapes formed by unidirectional fiber tows. Two types of plies, formed by many adjacent tapes, are typical of the FW process of an axisymmetric vessel: the hoop plies and the helical plies (see Fig. 2). Both of them are wound with a FW angle which is measured with respect to the cylinder and the tank axis, therefore, with respect to the meridian plane passing in each location of the wound tape. As depicted in Fig. 2, the hoop plies are formed by a continuous hoop winding of the CFRP tape. Instead, the complete helical layer is formed by two adjacent plies crossing with alternate positive and negative filament winding angles (i.e., one $+\alpha$ ply and one $-\alpha$ ply).

The multilayered layup consists of a 3.35-mm-thick aluminum layer and a 3.2-mm-thick multilayer CFRP. The connection is ensured by an adhesive layer whose nominal thickness is 0.12 mm. The mechanical properties of several materials obtained from manufacturer specifications are reported in Table 1 Instead, the stacking sequence obtained through the filament winding process is $[90_2/\pm 11/90_2/\pm 11/90_2/\pm 11/\pm 11/70_2]$. The nominal section of the cylindrical

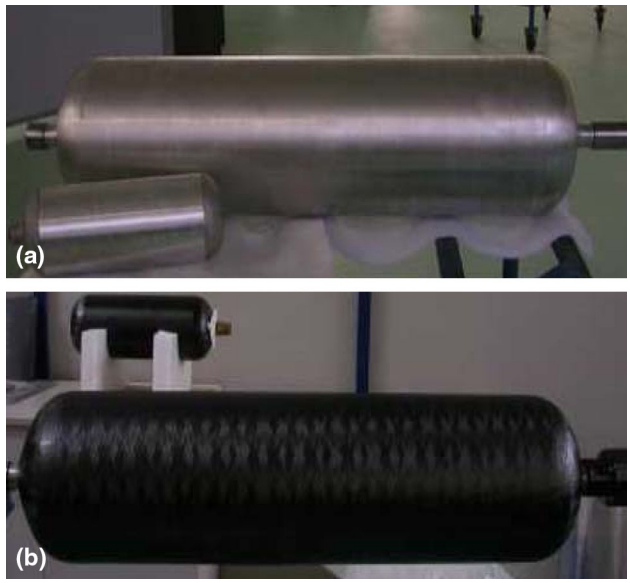

Fig. 1 Test article liner (a) and the whole structure obtained by filament winding process (b)

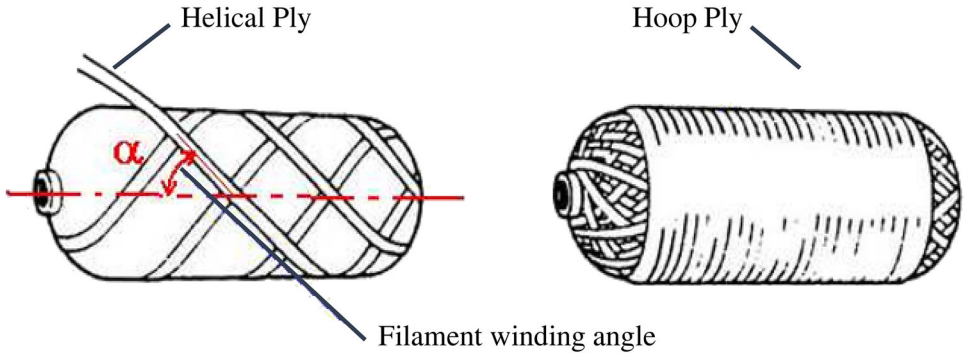

Fig. 2 Ply configuration adopted during filament winding process of an axisymmetric vessel. Helical plies ad hoop plies are used in combination to obtain the hollow structure

Table 1 Mechanical properties of aluminum layer (Al), composite material (CFRP) and adhesive layer (Ad)

	E_1, GPa	E_2, GPa	E_3, GPa	G_{12}, GPa	G_{13}, GPa	G_{23}, GPa	υ_{12}	υ_{13}	υ_{23}	ρ, Kg/m^3
Al	71	71	71	26.7	26.7	26.7	0.33	0.33	0.33	2700
CFRP	172	8.2	8.2	4.1	4.1	2.3	0.23	0.23	0.42	1520
Ad	2	2	2	7.6	7.6	7.6	0.30	0.30	0.30	1200

component shows an external radius of about 85 mm. The same bending radius is used to close the hollow structure on both tips.

The composite layup is maintenance critical because it represents the barrier between the liner and the environment. There the surface is randomly subject to impact with space debris, which may induce delamination between several plies. In addition, the energy released can affect the adhesive layer interface inducing debonding between metallic and composite parts. The latter hazard can seriously threaten the space mission. The disconnection enabled by the impact can lead to a strong stiffness reduction, and the structure is no longer able to withstand the operational loads within the whole mission envelope. In this context, two different issues deal with composite mechanics. The former is about predicting damage induced by a low-velocity impact within a composite material (Ref 39). The latter demand is to provide a diagnosis of the damage in a nondestructive way. An assessment procedure based on numerical models has been developed in order to verify the severity of an impact on the COPV. The procedure relies on detailed FE models simulating the effect of the impacts at different energies on the integrity of the vessel. The same virtual framework can furthermore be used to simulate the propagation of GWs within the medium and identify such a damage. The installation of an array of transducers/receivers on the external surface of the COPV is required in order to generate a set of high-frequency waves. They propagate through the medium with a typical velocity which depends upon the excited mode and the excitation frequency. Each transducer can generate a signal and record the structural response. The comparison between the response recorded on the whole structure and that recorded in case of damage can be used to characterize the hidden flaw. However, the detailed model including 3D approach to discretize the whole structure and the sensors may be quite expensive although it returns a high-fidelity response. Hence, the wave propagation in the hollow structure is investigated by simplified models and compared with measurements carried out on the COPV.

3. Wave Propagation in Hollow Structure

The setup envisioned for continuously monitoring the hollow structure is reported in Fig. 3. A sensor network consisting of lead zirconate titanate piezoelectric transducers (PZTs) is adopted to interrogate the cylindrical region. A couple of transducers are located along the radial direction with 120° angle. The configuration allows avoiding symmetric superposition in signal analysis while exciting the transducers separately to localize the damage. The longitudinal propagation is instead observed through a series of transducers along the rotational axis. That propagation is adopted to characterize and validate numerical frameworks and look into the wave damage interaction.

3.1 Experimental Setup

The experimental setup used to run laboratory tests is presented here to describe the datasets acquisition process which may be involved in the space application. In the latter case, the hardware will be optimized and designed to obtain a compact device (Ref 40, 41). On the contrary, the setup and the interrogation procedure are confirmed. Figure 4 shows the three PZT disks made of ferroelectric soft piezo material (PIC255) by Physik Instrumente which are bonded to the cylindrical surface along the longitudinal direction. The thickness of the transducer is 0.25 mm. A vacuum-based secondary bonding procedure commonly used by aircraft industries is used to obtain the optimum adhesion. The thin bonding layer obtained is used to transmit the deformation by an ultrasonic dry coupled method. Measurements are taken in a laboratory with uncontrolled environment. An arbitrary waveform generator (HP/Agilent 33120A) is used to generate a 4.5 cycle sinusoidal waveform with 10 Vpp amplitude in order to polarize the PZT disk. The number of cycles is chosen to obtain a good compromise between spectral bandwidth and time duration of the signal. The Hann window is adopted to prevent undue frequency leakage providing undesired effects due to dispersion.

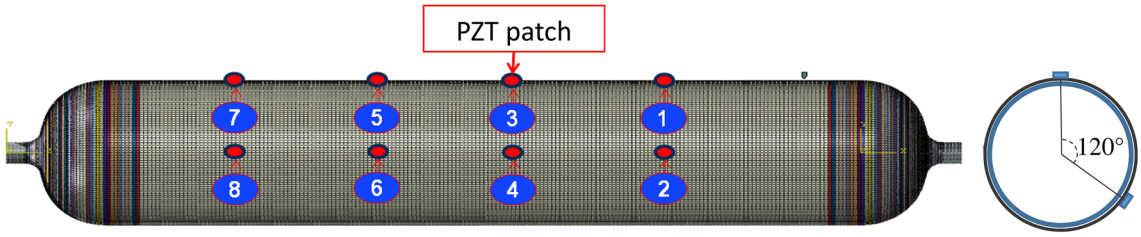

Fig. 3 Model setup for guided waves inspection of the hollow structure

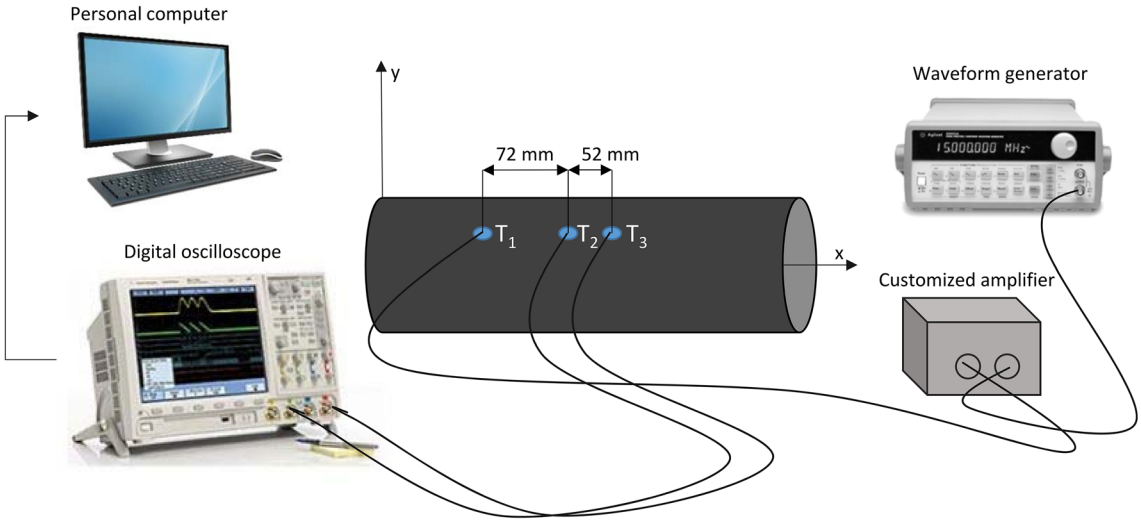

Fig. 4 Schematization of the overall experimental setup adopted for wave propagation analysis

The propagation is excited in the range 20-100 kHz to intercept the dispersive behavior of the first antisymmetric mode of Lamb waves (A_0). That is where the wave is mostly tuned with the PZT disk allowing its detection over the fundamental symmetric mode (S_0) in the time domain. To increase the signal-to-noise ratio, an amplifier is finally adopted to boost the voltage up to 80 Vpp. For every interrogation, the PZT disk selected as actuator (T_1) is excited using a burst of the generated signal with a time repetition period of 1 s. This interval is sufficient enough for the propagating wave to vanish before the subsequent interrogation. Ten repetitions are adopted to increase the signal-to-noise ratio again. Lamb waves generated by the converse piezoelectric effect travel through the structure. In a pitch catch configuration, they are then sensed by the remaining transducers (T_2 and T_3) due to the direct piezoelectric effect. When the transmitter is excited, the receivers are synchronized in order to compare the arrival time of recorded signals and intercept the propagation behavior. Signal acquisition is made with an Agilent DSO7104A 4-channel digital oscilloscope using 2 MHz sampling rate. Propagating waves sensed by the receivers are post-processed with a personal computer to derive the propagation velocity.

3.2 Numerical Simulation

Different FE models are built for this study for different purposes. Transient dynamic simulations are required since the phenomena under analysis are better analyzed in the time domain. Dynamic explicit techniques are adopted to integrate the equation of motion. A dedicated 3D model (see Fig. 5) can be used to catch all the component behaviors of interest

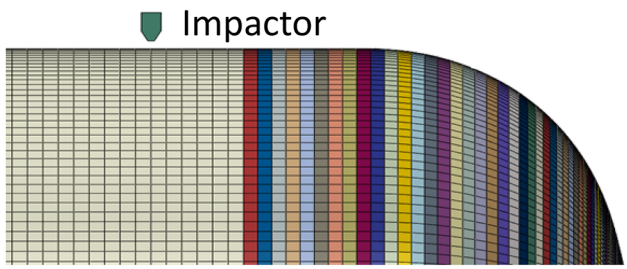

Fig. 5 3D model setup developed for Impact simulation. Although it can be used for wave propagation, it requires high computational costs

(damage, disbonding, transient response to transducers excitations) accounting for the geometric complexity of the COPV. In addition, due to the detailed discretization, the same model may be exploited to characterize the impact behavior (Ref 39).

Although the prescribed model returns a high-fidelity response, it does not allow an efficient strategy for simulating the wave propagation. As depicted in Fig. 6, the propagation along the line of sight can be idealized as a perturbation in a thin plate along the same direction. The latter assumption can be considered acceptable especially for relatively high radius of curvature. In addition, while looking into the wave propagation behavior, the idealization allows to control the echoes reflected at the free edges, without altering the characteristics of the direct propagating mode.

Since the model must be able to simulate the dynamic behavior of the structure at relatively high frequencies (50-

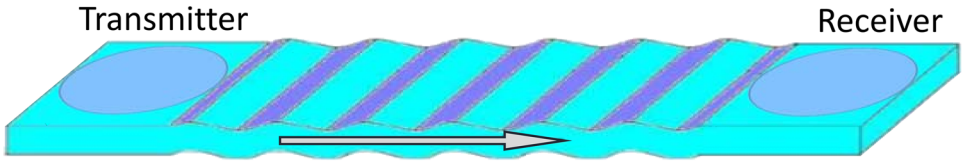

Fig. 6 Simplified propagation model for guided wave propagation along longitudinal direction. The wave propagating along a specific line of sight neglects the curvature of the solid medium in the other directions

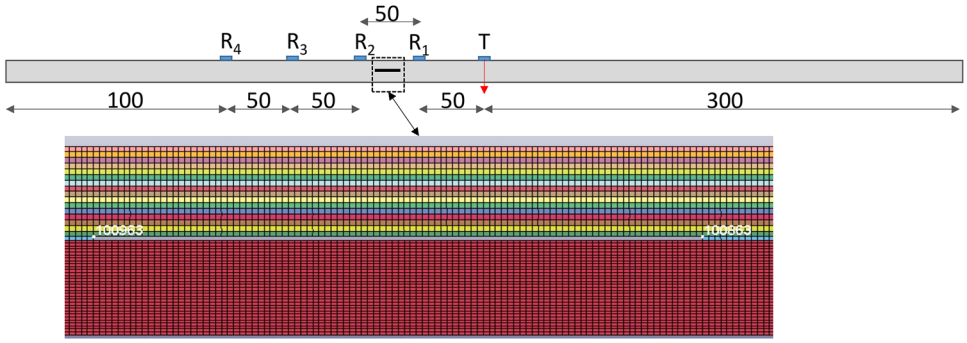

Fig. 7 2D plane strain model with disbonding. The debonding between metallic and composite layers is idealized removing the bonding layer. In that region, the discontinuity is due to the loss of structural continuity

100 kHz), one of the major challenges is the capability of the solver to handle very refined models. The dimension of the elements must be chosen to describe the wave shape with good approximation. Estimating the asymptotic velocity of the A_0 mode as 2000 m/s, the wavelength at 100 kHz can be calculated as $\lambda = \frac{v}{f} = \frac{2000}{100{,}000} \approx 20$ mm. As a consequence, an average mesh size of 0.5-1 mm is required in order to accurately describe the shortest wave (f = 100 kHz). That in-plane discretization would lead to quite expensive simulations even simplifying the vessel with a 3D plate model. Hence, to evaluate computational costs as well as accuracy of the results during simulations, different 3D and 2D techniques are investigated in a comparative analysis.

Firstly, as anticipated above, the full 3D discretization of a multilayered 600 × 600 mm^2 plate is adopted to idealize the structure and the propagation along the longitudinal direction of the vessel. Each layer is discretized as a single lamina, and the anisotropic properties are associated with the direction of the fibers as engineering constants. The C3D8R element is used to idealize the solid medium. The reduced integration allows to limit the computational costs. That is where the equation of motion is integrated in the elements' centroid sonly rather than solving the equation of motion at all nodes. There, the solution is obtained from the first-order shape function adopted. The accuracy of the results is ensured by the in-plane mesh, which is already refined enough to correctly reconstruct the minimum wavelength.

Secondly, to look into a 2D model CPE4R element is employed to idealize the solid medium as depicted in Fig. 7. The reduced integration is still adopted for the reason given above. In the case of a multilayered structure, the detailed 2D plane strain model is extremely useful to simulate the behavior of the wave under different damage patterns and to correlate the time-dependent signal to the failure mode with a very fast analysis. The number of elements is further reduced, by limiting the discretization to the section along the propagation path. In addition, the failure is easily described either removing elements in the defect area (see adhesive line in Fig. 7) or duplicating nodes between two consecutive layers of the layup.

Finally, the ESL technique with first shear deformation theory (FSDT) is adopted to idealize the 600 × 600 mm^2 plate. The 3D approach is here simplified by displacement approximation through the thickness and numerical compensation of the shear effects (Ref 42). Again, the reduced integration is preferred to limit the computational efforts by idealizing the solid media with the S4R elements.

An important issue while simulating guided waves with finite element approach deals with idealizing the piezoelectric transducer. In the present study, a punctual load is used to excite the wave propagation due to the small dimension of the PZT adopted with respect to the distances involved. The thickness is much smaller than the thickness of the media while the diameter is smaller enough than the receivers distance. The node at T_1 (centroid of the PZT) is loaded with an out-of-plane force. That is simulating the contraction of the PZT along that direction. Instead, the out-of-plane velocity is recorded at the receivers (T_2 and T_3) and compared during post-processing to calculate the group velocity.

4. Results

When the transducer is excited with a variable voltage, it may generate different waves which are categorized as symmetric or antisymmetric depending upon the particle motion with respect to the neutral axis/plane. They are traveling with a velocity that depends upon the mode and the thickness–frequency excited (Fig. 8). The analysis of the signal recorded at the receiver can provide useful information about the media along the line of sight. The time required for the excited wave to reach the target is referred as time of flight (ToF) and allows identifying the mode family of the incident wave. Moreover,

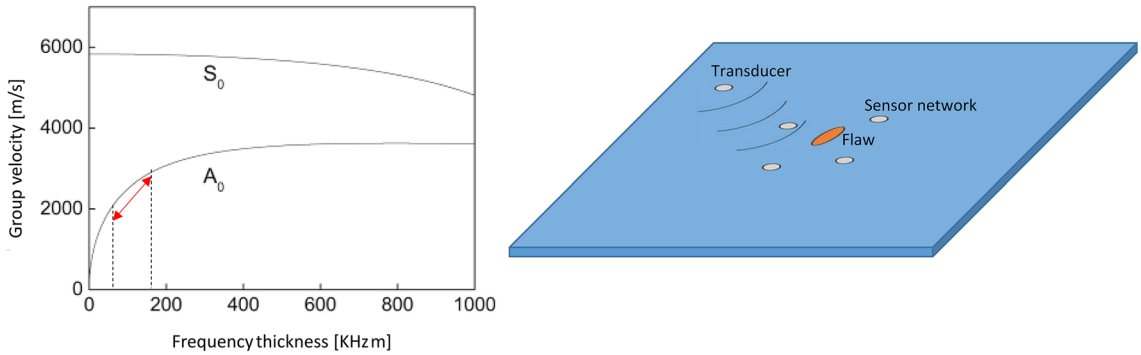

Fig. 8 Typical group velocities for symmetric and antisymmetric fundamental modes. The dispersion curves show the range of thickness–frequency where the velocity is rapidly changing. While the flaw appears, the waves crossing the defect behaves in a different manner

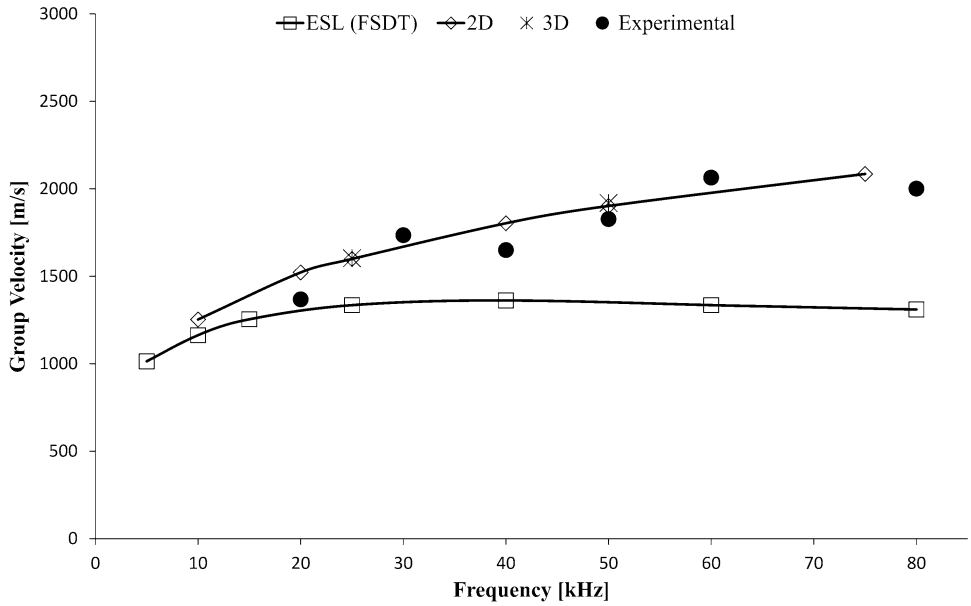

Fig. 9 Group velocities of propagating A_0 mode in composite aluminum plate. Measurements are compared with numerical outcomes using different discretization approaches. 3D and 2D approaches return quite close results whose error is negligible while compared to measurements. Instead, FSDT-based ESL approach is not accurate at higher frequencies

when a defect is occurring close to the wave path, the signal changes and the ToF is affected if the wave is dispersive (namely, the group velocity changes while varying the thickness–frequency).

The post-processing of the above information allows identifying the location of the flaw within the structure and eventually to calculate the extent of the damage. Coming to the space application, an impact-induced damage results in a discontinuity through the thickness, which corresponds to an abrupt change of the waveguide. The dispersion behavior of Lamb waves may result in a different arrival time due to the local interaction of the propagating wave packet with the flaw. Hence, it is worth knowing the dispersive properties of the specific media. The dispersion curve represents the group/phase velocity versus the frequency. It depicts the behavior of a specific mode traveling within a specific media (i.e., thickness, material, etc.). Such a damage modifies the effective thickness of the media and strongly affects the group velocity while the dispersion curve shows a gradient versus the section thickness (see Fig. 8). That velocity results from the ToF estimated between two sensors located at a known distance d as $v = d/$ ToF. Instead, the time of flight can be estimated from the characteristic time of two wave packets (t_1 and t_2) excited and/or sensed at two places. It can be calculated using signal processing techniques in both time domain and frequency domain and time–frequency domain. Among the techniques belonging to the third group, the short-time Fourier transform (STFT) can be used to define the characteristic time of a wave. The STFT of the digitized signal is:

$$\mathrm{STFT}\{x[n]\}(m,\omega) = X(m,\omega) = \sum_{n=-\infty}^{+\infty} x[n]\omega[n-m]e^{-j\omega m},$$

where $x[n]$ is the discrete signal and $\omega[n]$ is the windowing function. The Hann window is used to select a subset of a series of samples $[n]$ to be separately processed by Fourier transform (Ref 43). That function shows very low aliasing at the cost of a slightly decreased resolution due to the widening of the main lobe. The power spectral density (PSD) of the signal reconstructed by the STFT returns time and frequency simultane-

ously. The characteristic time is that associated with the maximum PSD. The difference $t_2 - t_1$ returns the time of flight. Then, the group velocity is directly estimated. The error expected using ToF calculation is connected to sampling frequency and distances between sensors' pair adopted to compare the characteristic time (Ref 44). Due to the setup employed, the error is estimated to be below 1% within the whole spectrum analyzed.

The results obtained post-processing experimental and numerical data are reported in Fig. 9. The group velocity is experimentally extracted at each frequency comparing characteristic time of the wave signals recorded at T_2 and T_3, respectively. Numerical curves are instead reconstructed considering the wave signals extracted at two sensors (d = 50 mm). As expected, the 3D approach predicts the dispersive behavior of the A_0 mode correctly. However, the computational cost is too expensive while structure complexity increases. It is worth noting how the ESL approach with first-order displacement theory is not able to predict the higher-frequency response. This is mostly due to the thickness of the

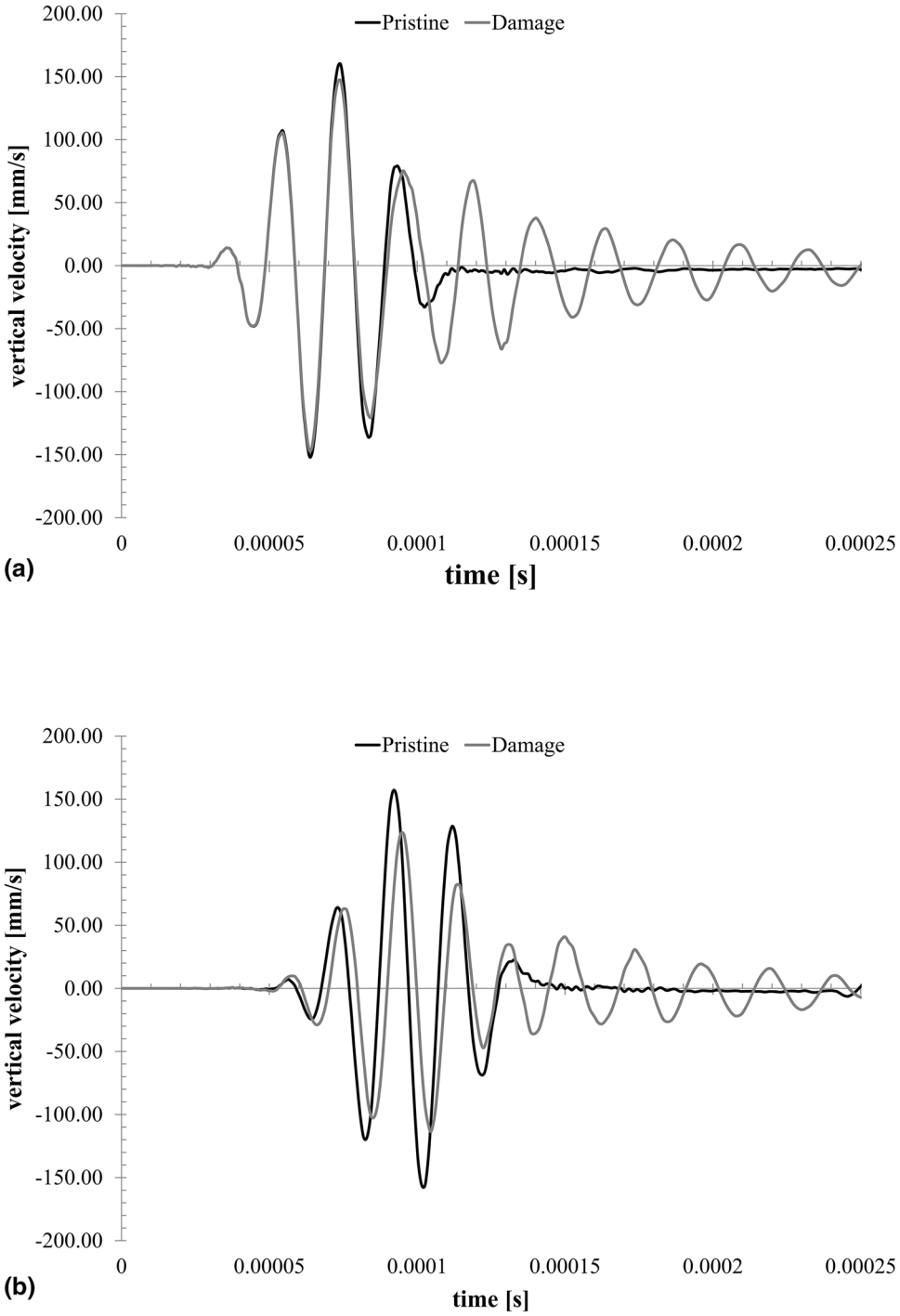

Fig. 10 Vertical velocity with and without flaw recorded at R_1 (a) and R_2 (b) idealizing the media with the 2D model. Carrier frequency fc = 50 kHz. The wave mostly excited is the A_0 mode while oscillating waves are emerging with the damage due to the trapped wave

structure which enables shear effects that cannot be predicted with a first-order shear deformation theory. Indeed, the slenderness factor of the plate does not suggest the use of this approach (Ref 45). This result is not acceptable even though the computational effort is strongly reduced. Otherwise, the 2D technique is able to predict the dispersive behavior of the A_0 mode with a lower computational cost possible.

For those reasons, the latter approach is selected for further investigating a possible debonding at the interface. A 20-mm disconnection is included in the numerical model by removing the bonding layer (see Fig. 7). The time histories recorded at R_1 (just before the damage) and R_2 (just after the damage) are compared to those obtained from the pristine structure. A clear example is depicted in Fig. 10. The signal acquired in pitch catch mode at 50 kHz is changing when the wave crosses the damage (b). Meanwhile, the direct A_0 mode is slightly affected when the wave is sensed before the damage (a). The amplitude of the antisymmetric mode is increasing because the induced delamination locally reduces the medium thickness and the structural impedance accordingly. Likewise, the ToF is increas-

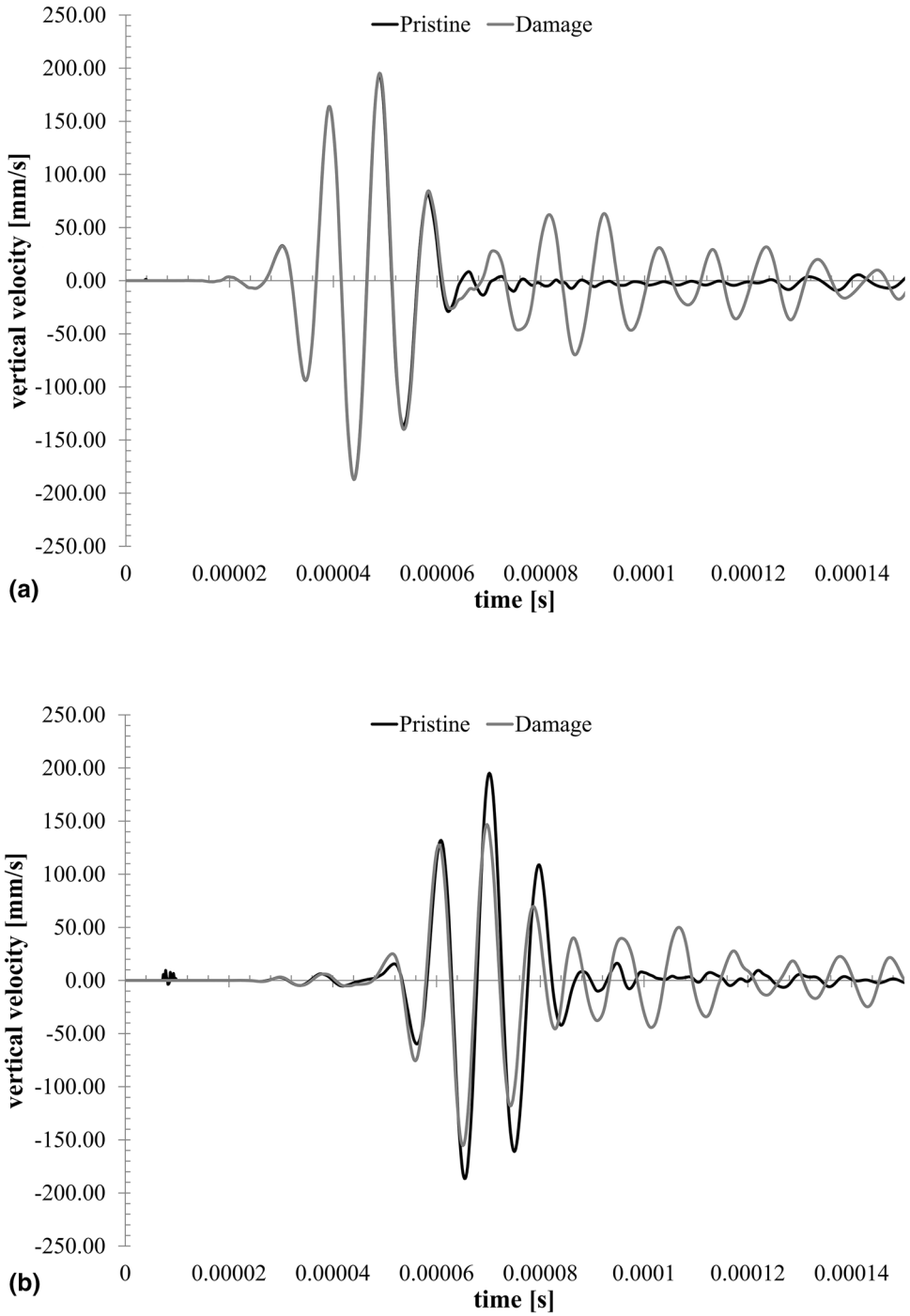

Fig. 11 Vertical velocity with and without flaw recorded at R_1 (a) and R_2 (b) idealizing the media with the 2D model. Carrier frequency fc = 100 kHz. The wave mostly excited is the A_0 mode while oscillating waves are emerging with the damage due to the trapped wave

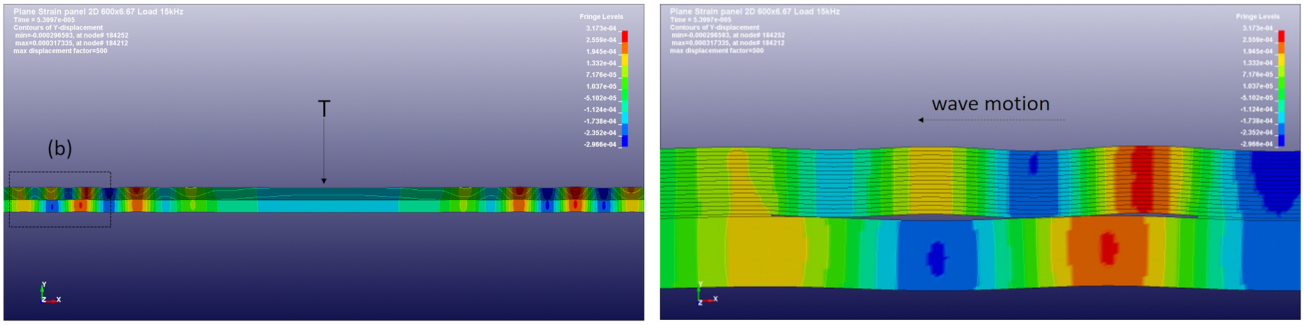

Fig. 12 Wavefield captured at 100 kHz. The line slip can be observed looking into the right side propagation (a). Simultaneously, the effect of the debonding is showed on the left side (a). The wave splits into two wave packets and it speeds up traveling in the down media as evident from the magnified wavefield (b)

ing due to such a reduction in the effective thickness. Namely, the thickness–frequency is decreasing and wave velocity decreases accordingly (see the A_0 trend in Fig. 9). Otherwise, in both cases the echoes are scattered back (a) or forward (b) from the damage location. The latter evidence is due to the trapped energy within the damage region which acts as a sort of "impedance cage." The wave transmitted through the first edge of the debonding is partially transmitted through the second edge. Instead, the wave reflected at the second edge is scattered back to the first edge. Here, the wave scattering is enabled again. This phenomenon results in the oscillation visible in the time history after the A_0 mode similarly to what happens when ice or another abrupt discontinuity is encountered (Ref 46). The same discussion can be argued looking into the signals recorded at R_3 and R_4 omitted here for the sake of the conciseness.

Instead, a different discussion can be made looking into the signals recorded while exciting a 100 kHz wave. Firstly, Fig. 11(a) shows that the A_0 is not perturbed at all. This is due to the lower wavelength which attenuates the interaction with damage visible in R_1. Secondly, Fig. 11(b) shows that the ToF is slightly affected due to the quite flat trend of the dispersion curve at that frequency. Thirdly, the oscillating waves appearing with damage have a shape similar to the excited wave. The latter evidence demonstrates that they are due to the waves trapped in the damage region and scattered back (a) or forward (b) at every rebound. Otherwise, the wave amplitude is still decreased at R_2 due to the impedance reduction. It is worth noting that a damage index approach can be used to detect the debonding with guided waves excited on the outer surface.

The complex wave interaction with damage is emphasized in Fig. 12 which depicts the wave field captured at 100 kHz (vertical displacement).

Figure 12(a) shows the propagation in both directions of the plate. On the right side, the upper (composite) and lower (metal) parts are perfectly bonded. There, the wave excited on the upper surface is traveling with the same velocity in the whole thickness. However, a slightly attenuation is visible in the lower part due to the adhesive layer and medium discontinuity. The structural impedance is constant in the upper as well as in the lower section with a step at the bonding layer which acts as a sort of "slip line." On the left side, the upper (composite) and lower (metal) parts are disconnected due to debonding. Until there, the wave excited on the upper surface is traveling with the same velocity in the whole thickness showing a slight attenuation due to the slip line again. However, at the debonding edge the wave splits into two waves traveling in the upper and lower section, respectively. Those waves show a completely different velocity due to the different properties of the media. In detail, the wave packet speeds up while traveling in the down media. This phenomenon is highlighted in Figure 12(b) which depicts the magnification of the wave field at the debonding location. There the presence of the slip line is hidden by the interaction phenomena.

5. Concluding Remarks

Structural diagnosis through active acousto-ultrasonics approach where PZT is employed for actuation and sensing guided waves is efficiently adopted for monitoring composite structures. The complex propagation behavior in multilayered media requires simulation to predict its key characteristics. This paper demonstrates that simulation can be adopted to predict the dispersive behavior of the first antisymmetric mode of Lamb waves (A_0). In addition, computational costs can be reduced without compromising accuracy by using 2D plain strain discretization at the cost of analyzing one propagation direction per simulation. Although the FSDT-based ESL approach reduces strongly the computational efforts incorporating the whole in-plane propagation, the result is not accurate enough. The 2D model is then used to reveal the interaction of GWs with a debonding. It is worth noting how the wave is scattered at the flaw in a way depending upon the frequency. At 50 kHz, the wave crossing the defect shows a reduced amplitude due to the reflected energy. In addition, the time of flight increases and oscillating waves are emerging due to the "impedance cage." Instead, at 100 kHz the wave amplitude decreases, but the time of flight is slightly affected. Oscillations due to the impedance cage are again present, and they appear well shaped. On top of that, the different material properties create a slip line at the bonding where the propagating wave is scattered through the thickness. Finally, the wave field shows that the wave splits into two wave packets at the debonding edge and it speeds up traveling in the down media. Although a deeper investigation is needed, all those phenomena can be adopted to reveal, localize and characterize the damage.

Acknowledgments

The present work received funding from STEPS program—Systems and Technologies for Space Exploration—a research project co-financed by Regione Piemonte (Piedmont Region) within the Phase 2 of P.O.R.-F.E.S.R. 2007-2013 EC program.

References

1. W. Fan and P. Qiao, Vibration-Based Damage Identification Methods: A Review and Comparative Study, *Struct. Health Monit.*, 2011, **10**(1), p 83–111
2. J. Moll, K. Bechtel, B. Hils, and V. Krozer, Mechanical vibration sensing for structural health monitoring using a millimeter-wave Doppler radar sensor. *Proceedings of the 7th European Workshop on Structural Health Monitoring*, 2014, p. 1802–1808
3. K. Neuschwander, J. Moll, V. Memmolo, M. Schmidt, and M. Bücker, Simultaneous Load and Structural Monitoring of a Carbon Fiber Rudder Stock: Experimental Results from a Quasi-Static Tensile Test, *J. Intell. Mater. Syst. Struct.*, 2019, **30**(2), p 272–282
4. M. Mitra and S. Gopalakrishnan, Guided Wave Based Structural Health Monitoring: A Review, *Smart Mater. Struct.*, 2016, **25**(5), p 053001
5. V. Memmolo, F. Ricci, N.D. Boffa, L. Maio, and E. Monaco, Structural Health Monitoring in Composites Based on Probabilistic Reconstruction Techniques, *Proc. Eng.*, 2016, **167**, p 48–55
6. L. Maio, V. Memmolo, S. Boccardi, C. Meola, F. Ricci, N.D. Boffa, and E. Monaco, Ultrasonic and IR Thermographic Detection of a Defect in a Multilayered Composite Plate, *Proc. Eng.*, 2016, **167**, p 71–79
7. G. Cottone, S. Gollwitzer, U. Heckenberger, and D. Straub, Reliability-oriented optimization of replacement strategies for monitored composite panels for aircraft structures. *Proceedings of the 9th International Workshop on Structural Health Monitoring*, 2013, 2, p. 2728–2735
8. I. Ursu, D. Enciu, and A. Toader, Towards Structural Health Monitoring of Space Vehicles, *Aircr. Eng. Aerosp. Technol.*, 2017, **89**(6), p 920–927
9. L. De Marchi, A. Marzani, J. Moll, P. Kudela, M. Radzieński, and W. Ostachowicz, A pulse Coding and Decoding Strategy to Perform Lamb Wave Inspections Using Simultaneously Multiple Actuators, *Mech. Syst. Signal Process.*, 2017, **91**, p 111–121
10. D. Chronopoulos, Calculation of Guided Wave Interaction with Nonlinearities and Generation of Harmonics in Composite Structures Through a Wave Finite Element Method, *Compos. Struct.*, 2018, **186**, p 375–384
11. H. Cho, M. Hasanian, S. Shan, and C.J. Lissenden, Nonlinear Guided Wave Technique for Localized Damage Detection in Plates with Surface-Bonded Sensors to Receive Lamb Waves Generated by Shear-Horizontal Wave Mixing, *NDT E Int.*, 2019, **102**, p 35–46
12. G.P.M. Fierro and M. Meo, Nonlinear Elastic Imaging of Barely Visible Impact Damage in Composite Structures Using a Constructive Nonlinear Array Sweep Technique, *Ultrasonics*, 2018, **90**, p 125–143
13. G.P.M. Fierro and M. Meo, A combined Linear and Nonlinear Ultrasound Time-Domain Approach for Impact Damage Detection in Composite Structures Using a Constructive Nonlinear Array Technique, *Ultrasonics*, 2019, **93**, p 43–62
14. N.P. Yelve, M. Mitra, and P.M. Mujumdar, Detection of Delamination in Composite Laminates Using Lamb Wave Based Nonlinear Method, *Compo. Struct.*, 2017, **159**, p 257–266
15. B. Yang, F.Z. Xuan, S. Chen, S. Zhou, Y. Gao, and B. Xiao, Damage Localization and Identification in WGF/Epoxy Composite Laminates by Using Lamb Waves: Experiment and Simulation, *Compos. Struct.*, 2017, **165**, p 138–147
16. V. Memmolo, N.D. Boffa, L. Maio, E. Monaco, and F. Ricci, Damage Localization in Composite Structures Using a Guided Waves Based Multi-Parameter Approach. Aerospace, 2018, 5, art. No 111
17. Z. Tian, L. Yu, and C. Leckey, Delamination Detection and Quantification on Laminated Composite Structures with LAMB Waves and Wavenumber Analysis, *J. Intell. Mater. Syst. Struct.*, 2015, **26**(13), p 1723–1738
18. O. Mesnil, C.A. Leckey, and M. Ruzzene, Instantaneous and Local Wavenumber Estimations for Damage Quantification in Composites, *Struct. Health Monit.*, 2015, **14**(3), p 193–204
19. C.C. Tao, H.L. Ji, J.H. Qiu, C. Zhang, Z. Wang, and W. Yao, Characterization of Fatigue Damages in Composite Laminates Using Lamb Wave Velocity and Prediction of Residual Life, *Compos. Struct.*, 2017, **166**, p 219–228
20. M. Deng and J. Pei, Assessment of Accumulated Fatigue Damage in Solid Plates Using Nonlinear Lamb Wave Approach, *Appl. Phys. Lett.*, 2007, **90**, p 121902
21. V. Memmolo, E. Monaco, N.D. Boffa, L. Maio, and F. Ricci, Guided Wave Propagation and Scattering for Structural Health Monitoring of Stiffened Composites, *Compos. Struct.*, 2018, **184**, p 568–580
22. T. Wandowski, P. Kudela, and W.M. Ostachowicz, Numerical Analysis of Elastic Wave Mode Conversion on Discontinuities, *Compos. Struct.*, 2019, **215**, p 317–330
23. C. Schaal, H. Samajder, H. Baid, and A. Mal, Rayleigh to Lamb Wave Conversion at a Delamination-Like Crack, *J. Sound Vib.*, 2015, **353**, p 150–163
24. E. Glushkov, N. Glushkova, M.V. Golub, J. Moll, and C.P. Fritzen, Wave Energy Trapping and Localization in a Plate with a Delamination. *Smart Mater. Struct.*, 2012, **21**(12), art. no. 125001
25. J. Moll, Damage Localization in Composite Structures with Smoothly Varying Thickness Based on the Fundamental Antisymmetric Adiabatic Wave Mode, *Ultrasonics*, 2016, **71**, p 111–114
26. L. Maio, V. Memmolo, F. Ricci, N.D. Boffa, and F. Ricci, Investigation on Fundamental Modes of Guided Waves Propagating in Symmetric and Nonsymmetric Composite Laminates, *Proc. Inst. Mech. Eng. Part C*, 2017, **231**(16), p 2988–3000
27. A.J. Croxford, J. Moll, P.D. Wilcox, and J.E. Michaels, Efficient Temperature Compensation Strategies for Guided Wave Structural Health Monitoring, *Ultrasonics*, 2010, **50**(4-5), p 517–528
28. V. Memmolo, N. Pasquino, and F. Ricci, Experimental Characterization of a Damage Detection and Localization System for Composite Structures, *Meas. J. Int. Meas. Confed.*, 2018, **129**, p 381–388
29. J. Moriot, N. Quaegebeur, A.L. Duff, and P. Masson, A Model-Based Approach for Statistical Assessment of Detection and Localization Performance of Guided Wave-Based Imaging Techniques, *Struct. Health Monit.*, 2018, **17**(6), p 1460–1472
30. Y. Shen and V. Giurgiutiu, Combined Analytical FEM Approach for Efficient Simulation of Lamb Wave Damage Detection, *Ultrasonics*, 2016, **69**, p 116–128
31. V. Thierry, L. Brown, and D. Chronopoulos, Multi-scale Wave Propagation Modelling for Two-Dimensional Periodic Textile Composites, *Compos. B Eng.*, 2018, **150**, p 144–156
32. R.T. Schulte, C.P. Fritzen, and J. Moll, Spectral Element Modelling of Wave Propagation in Isotropic and Anisotropic Shell-Structures Including Different Types of Damage. *IOP Conf. Ser. Mater. Sci. Eng.*, 2014, **2014**(1), art. no. 012065
33. E. Rosenkrantz, A. Bottero, D. Komatitsch, and V. Monteiller, A Flexible Numerical Approach for Non-destructive Ultrasonic Testing Based on a Time-Domain Spectral-Element Method: Ultrasonic Modeling of Lamb Waves in Immersed Defective Structures and of Bulk Waves in Damaged Anisotropic Materials, *NDT E Int.*, 2019, **101**, p 72–86
34. M.V. Golub, A.N. Shpak, I. Muller, and C.P. Fritzen, Numerical Simulation of Lamb Wave Excitation by the Partially Debonded Rectangular Strip-Like Piezoelectric Actuator Based on the Integral Approach and hp-FEM. *Proc. Int. Conf. Days Diffr.,* 2016, art. no. 7756836, p. 171–176
35. L. Maio, F. Franco, A. Squillace, and L. Lecce, A Simplified Approach to Numerical Simulation of LFW Process of Ti6Al4 V Alloy: Investigation on Friction and Temperature, *Int. J. Adv. Manuf. Technol.*, 2016, **86**(9-12), p 3217–3228
36. L. Maio, S. Ameduri, A. Concilio, E. Monaco, V. Memmolo, and F. Ricci, Development of a De-Icing System for Aerodynamic Surfaces Based on Ultrasonic Waves. *Proc. SPIE Int. Soc. Opt. Eng.*, 2018, 10600, art. no. 106000H
37. S. Sorohan, N. Constantin, M. Găvan, and V. Anghel, Extraction of Dispersion Curves for Waves Propagating in Free Complex Waveguides by Standard Finite Element Codes, *Ultrasonics*, 2011, **51**(4), p 503–515
38. C. Schaal, S. Zhang, H. Samajder, and A. Mal, An Analytical Study of the Scattering of Ultrasonic Guided Waves at a Delamination-Like

Discontinuity in a Plate, *Proc. Inst. Mech. Eng. Part C*, 2017, **231**(16), p 2947–2960
39. L. Maio, E. Monaco, F. Ricci, and L. Lecce, Simulation of Low Velocity Impact on Composite Laminates with Progressive Failure Analysis, *Compos. Struct.*, 2013, **103**, p 75–85
40. K. Neuschwander, A. Shrestha, J. Moll, V. Krozer, and M. Bücker, Multichannel Device for Integrated Pitch Catch and EMI Measurements in Guided Wave Structural Health Monitoring Applications, *Proceedings of the 11th International Workshop on Structural Health Monitoring*, 2017, 1, p 1723–1730
41. V. Memmolo, L. Maio, E. Monaco, N. Ciminiello, and B. Di Giampaolo, A Multi-channel System for On-line Structural Health Monitoring using Guided Waves, *Proceedings of the IEEE International Workshop on Metrology for Aerospace*, 2019
42. R.D. Mindlin, Influence of Rotary Inertia and Shear on Flexural Motions of Isotropic Elastic Plates, *J. Appl. Mech. Trans. ASME*, 1951, **18**, p 31–38
43. F.J. Harris, On the Use of Windows for Harmonic Analysis with the Discrete Fourier Transform, *Proc. IEEE*, 1978, **66**(1), p 51–83
44. L. Maio, F. Ricci, V. Memmolo, E. Monaco, and N.D. Boffa, Application of Laser Doppler Vibrometry for Ultrasonic Velocity Assessment in a Composite Panel with Defect, *Compos. Struct.*, 2018, **184**, p 1030–1039
45. Abaqus 6.12 Analysis User's Guide
46. V. Memmolo and J. Moll, Guided Wave Propagation and Interaction with Ice Layers in Marine Structures, *Proceedings of the 8th European Workshop on Structural Health Monitoring, ndt.net*, 2018, 23, 11, p 1–8